Pergamon

Int. Comm. Heat Mass Transfer, Vol. 24, No. 6, pp. 805–814, 1997
Copyright © 1997 Elsevier Science Ltd
Printed in the USA. All rights reserved
0735-1933/97 $17.00 + .00

PII S0735-1933(97)00067-5

SIMILARITY SOLUTIONS FOR BUOYANCY-INDUCED FLOW OF A POWER-LAW FLUID OVER A HORIZONTAL SURFACE IMMERSED IN A POROUS MEDIUM

Ali J. Chamkha
Department of Mechanical and Industrial Engineering
Kuwait University
Safat, 13060 - KUWAIT.

(Communicated by J.P. Hartnett and W.J. Minkowycz)

ABSTRACT

Continuum equations governing steady, laminar, buoyancy-induced flow and heat transfer of a power-law fluid over a horizontal surface immersed in a uniform porosity and permeability porous medium are developed. These partial differential equations are transformed into ordinary differential equations by using a general similarity transformation for variable surface temperature and constant heat flux cases. The resulting equations are solved numerically by an implicit finite-difference method. Numerical results for typical velocity and temperature profiles are presented and discussed. © 1997 Elsevier Science Ltd

Introduction

There have been considerable interest in studying natural or buoyancy-induced flows in fluid-saturated porous media adjacent to surfaces in recent years. This interest stems from numerous possible industrial and technological applications. Examples of some applications include geothermal reservoirs, drying of porous solids, heat exchanger design, petroleum production, filtration, chemical catalytic reactor, nuclear waste repositories, and geophysical flows. The prediction and knowledge of heat transfer rate and temperature distribution from a heated horizontal surface to surrounding ground water in a subsurface environment has important applications in the assessment of geothermal resources and the design of a geothermal power plant [1]. This paper considers steady, laminar buoyancy-induced flow of a non-Newtonian power-law fluid over a semi-infinite horizontal surface embedded in a uniform porous medium. Most studies on flow in porous media have been concentrated on Newtonian fluids (see, for instance, Cheng and Chang [2], Nakayama and Koyama [3], Govindarajullu and Moorthy [4], and Chamkha [5]). Cheng and Chang [2] have used a similarity transformation in solving free convection flow from a horizontal surfaces in porous media while Nakayama and Koyama [3] have employed the Karman-Pohlhausen approximate integral method. Chamkha [5] have considered free convection from a cone and a wedge in porous media. Chamkha [5] have employed a similarity transformation for the case of variable surface temperature.

Inspite of the frequent occurrence of industrial applications using non-Newtonian fluids such as fossil fuels, molten plastics, polymer solutions, dyes, varnishes, suspensions, paints, and multi-grade oil, there have been little work done on non-Newtonian flows in porous media. Some of this work can be found in the papers by Chen and Chen [6,7], Nakayama and Koyama [8] and Chamkha [9,10]. Chen and Chen [6,7] have obtained solutions for free convection non-Newtonian fluid flows over a vertical plate, horizontal circular cylinder, and a sphere embedded in a porous medium. Nakayama and Koyama [8] have generalized the work of Chen and Chen [6, 7] to non-isothermal bodies of arbitrary shape. Chamkha [9, 10] have considered steady and transient non-Newtonian fluid flow in a porous medium channel. Recently, Metha and Rao [1] have studied buoyancy-induced flow of non-Newtonian fluids over a non-isothermal horizontal plate embedded in a porous medium using a similarity transformation.

Motivated by the works mentioned earlier especially that of Metha and Rao [1], it is of interest in this paper to extend the problem of Metha and Rao [1] to the case of uniform wall heat flux. A general similarity transformation procedure is obtained. The thermophysical properties of the non-Newtonian fluid such as the power-law index are assumed constant .

Problem Formulation

Consider steady, laminar, buoyancy-induced boundary-layer flow of a non-Newtonian power-law fluid in a uniform porous medium supported by a horizontal flat surface as shown in Fig. 1. The governing equations for this investigation are based on the balance laws of mass, linear momentum, and

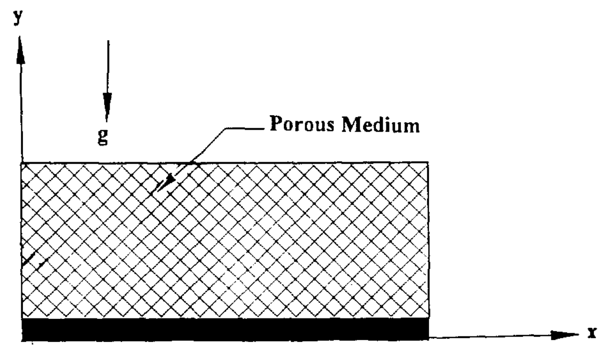

FIG. 1

Schematic of the Problem

energy modified to include the effect of the presence of the porous medium and the buoyancy and non-Newtonian fluid effects. The model proposed by Christopher and Middleman [11], and Dharmadhikari and Kale [12] for non-Newtonian power-law fluid flow in a porous medium along with the boundary-layer and Boussinesq approximation are employed herein. The resulting equations can be written as (see, Mehta and Rao [1]):

$$\frac{\partial u}{\partial x}+\frac{\partial v}{\partial y}=0 \tag{1}$$

$$\frac{\partial u^n}{\partial y}=-\frac{\rho K g\beta}{\mu}\frac{\partial T}{\partial x} \tag{2}$$

$$u\frac{\partial T}{\partial x}+v\frac{\partial T}{\partial y}=\alpha\frac{\partial^2 T}{\partial y^2} \tag{3}$$

where x and y are the horizontal and normal distances, respectively. u, v, and T are the x-component of velocity, y-component of velocity, and temperature, respectively. ρ and α are the fluid density and the medium effective thermal diffusivity, respectively. K, μ and n are the porous medium modified permeability, the power-law fluid constant and index, respectively. β and g are the coefficient of volumetric thermal expansion and the gravitational acceleration, respectively.

Christopher and Middleman [11] and Dharmadhikari and Kale [12] have reported expressions for the modified permeability coefficient K for a non-Newtonian fluid in a porous packed bed of spherical particles. These expressions are

$$K(n)=\begin{cases}\dfrac{6}{25}\left(\dfrac{n\varepsilon}{3n+1}\right)^n\left(\dfrac{\varepsilon d}{3(1-\varepsilon)}\right)^{n+1} & \text{(Christopher and Middleman [11])}\\[2ex] \dfrac{2}{\varepsilon}\left(\dfrac{d\varepsilon^2}{8(1-\varepsilon)}\right)^{n+1}\left(\dfrac{6n+1}{10n-3}\right)\left(\dfrac{16}{75}\right)^{3(10n-3)/(10n+11)} & \text{(Dharmadhikari and Kale[12])}\end{cases} \tag{4}$$

where d and ε are the particle diameter and the medium porosity, respectively.

The physics of the problem suggests the following boundary conditions

$$\begin{aligned}&v(x,0)=0, \quad T(x,0)=T_w(x) \quad \text{or} \quad q_w=\text{constant}\\ &u(x,\infty)=0, \quad T(x,\infty)=T_\infty\end{aligned} \tag{5}$$

where $T_w(x)$ is the variable wall temperature, q_w is the wall heat flux, and T_∞ is the ambient fluid temperature.

It is convenient to nondimensionalize Eqs. (1) - (3) by employing the following equations

$$
\begin{aligned}
x &= XL, \qquad y = YL\,Ra^{-1/3}, \qquad u = u_c F \\
v &= u_c Ra^{-1/3} G, \qquad T = T_\infty + HT_c\,, \qquad u_c = \frac{\alpha Ra^{2/3}}{L}
\end{aligned}
\tag{6}
$$

where L is a characteristic length, T_c is a characteristic temperature, and Ra is the modified Rayleigh number. The characteristic temperature and the modified Rayleigh number take on the respective forms:

$$
T_c = \begin{cases} T_w - T_\infty & \text{constant wall temperature} \\ T_r - T_\infty & \text{variable wall temperature} \\ \dfrac{q_w L}{k R_a^{1/3}} & \text{constant wall heat flux} \end{cases}
\tag{7}
$$

$$
Ra = \begin{cases} (\dfrac{L}{\alpha})^{3n/(2n+1)} (\dfrac{\rho K g \beta (T_w - T_\infty)}{\mu})^{3/(2n+1)} & \text{constant wall temperature} \\ (\dfrac{L}{\alpha})^{3n/(2n+1)} (\dfrac{\rho K g \beta (T_r - T_\infty)}{\mu})^{3/(2n+1)} & \text{variable wall temperature} \\ (\dfrac{L}{\alpha})^{3n/(2n+2)} (\dfrac{\rho K g \beta q_w L}{\mu k})^{3/(2n+2)} & \text{constant wall heat flux} \end{cases}
\tag{8}
$$

where T_r and k are reference wall temperature and the porous medium thermal conductivity, respectively.

Substituting Eqs. (6)-(8) into Eqs. (1)-(3) and (5) results in the following dimensionless equations and conditions

$$
\frac{\partial F}{\partial X} + \frac{\partial G}{\partial Y} = 0 \tag{9}
$$

$$
\frac{\partial F^n}{\partial Y} = - \frac{\partial H}{\partial X} \tag{10}
$$

$$
F\frac{\partial H}{\partial X} + G\frac{\partial H}{\partial Y} = \frac{\partial^2 H}{\partial Y^2} \tag{11}
$$

$$
\begin{aligned}
&G(X,0) = 0, \quad H(X,0) = H_w(X) = X^\lambda \ \text{ or } \ \frac{\partial H}{\partial Y}(X,0) = -1 \\
&F(X,\infty) = 0 \quad H(X,\infty) = 0
\end{aligned}
\tag{12}
$$

It should be noted that a power-law function for wall temperature distribution has been employed for the variable wall temperature case with λ being a constant.

It is of interest in the present work to determine the appropriate transformations for the three thermal cases mentioned before which lead to similarity solutions. A general procedure is outlined below.

Let

$$F = \frac{\partial\psi}{\partial Y} \quad , \quad G = -\frac{\partial\psi}{\partial X} \quad , \quad \xi = X$$
$$\eta = X^a Y \quad , \quad \psi = X^b f(\eta) \quad , \quad H = X^c \theta(\eta) \tag{13}$$

where ψ is the stream function and a, b, and c are constants to be determined. Using Eqs. (13), it can be shown that

$$F = X^{a+b} f' \quad , \quad G = -X^{b-1}(a\eta f' + bf) \tag{14}$$

where a prime denotes ordinary differentiation with respect to η.

Substituting Eqs. (13) and (14) into Eqs. (9)-(11) results in the following equations

$$((f'')^n)' + X^{c-1-a(n+1)-nb}(a\eta\theta' + c\theta) = 0 \tag{15}$$

$$\theta'' + X^{b-a-1}(bf\theta' - cf'\theta) = 0 \tag{16}$$

For a similar solution, the following conditions

$$c - 1 - a(n+1) - nb = 0 \tag{17}$$

$$b - a - 1 = 0 \tag{18}$$

must be satisfied.

Constant Wall Temperature:

For this special case, H(X,0) =1 which requires that c = 0. With c = 0, Eqs. (17) and (18) yield

$$a = \frac{-(n+1)}{2n+1} \quad , \quad b = \frac{n}{2n+1} \tag{19}$$

Variable Power-Law Wall Temperature:

For a non-isothermal plate, the boundary condition for the fluid temperature at the wall is assumed to be $H(X,0) = X^{\lambda}$. Comparing this with Eq. (13f) gives $c = \lambda$. This yields the following solutions for a and b

$$a = \frac{\lambda - (n+1)}{2n+1} \quad , \quad b = \frac{\lambda + n}{2n+1} \tag{20}$$

It can be seen that when λ is equated to zero (constant wall temperature), Eqs. (19) are recovered. It should be mentioned that Eqs. (20) and Eqs. (13) are the same as those employed by Mehta and Rao [1].

Constant Wall Heat Flux:

If the boundary is maintained at a constant heat flux, transforming Eq. (12c) by using Eqs. (13) produces the following similarity condition

$$a + c = 0 \tag{21}$$

For this case Eqs. (17), (18) and (21) can be solved for a, b, and c to give

$$a_1 = -(n+1) + \sqrt{n(n+1)}\ , \quad b_1 = -n + \sqrt{n(n+1)}, \quad c_1 = (n+1) - \sqrt{n(n+1)} \tag{22}$$

$$a_2 = -(n+1) - \sqrt{n(n+1)}, \quad b_2 = -n - \sqrt{n(n+1)}, \quad c_2 = (n+1) + \sqrt{n(n+1)} \tag{23}$$

It can be seen from Eqs. (22) and (23) that there exist two solutions for each of a, b, and c which satisfy Eqs. (17), (18), and (21) and lead to the same form of the similarity equations:

$$((f')^n)' + a\eta\theta' + c\theta = 0 \tag{24}$$

$$\theta'' + bf\theta' - cf'\theta = 0 \tag{25}$$

It should be mentioned that non-unique solutions of this kind were reported earlier by Ridha [13] in his work on three-dimensional mixed convection laminar boundary layer near a plane of symmetry.

The transformed boundary conditions become

$$\begin{aligned} &f(0) = 0\ , \quad \theta(0) = 1 \quad \text{or} \quad \theta'(0) = -1 \\ &f'(\infty) = 0, \quad \theta(\infty) = 0 \end{aligned} \tag{26}$$

Results and Discussion

Equations (24) and (25) subject to Eqs. (26) represent a nonlinear boundary-value problem which possesses no closed-form solution for all of the three cases discussed earlier. Therefore, it must be solved numerically. An implicit, iterative, tridiagonal finite-difference method similar to that discussed by Blottner [14] and Patankar [15] has been chosen for that purpose. In this method, the equations are discretized using three-point central difference quotients which are then converted into linear algebraic equations. The resulting tri-diagonal matrix of the algebraic equations is then solved by the Thomas' algorithm (see, Blottner [14]). Numerical difficulties were encountered when small computational domain was chosen. The problem required very fine grids. For this reason the computational domain consisted of 100,000 nodal points and a constant step size in η ($\Delta\eta$ = 0.00005) was used in the present work. The combination of the number of nodal points and the step size were selected after many numerical experimentations performed to assess grid independence and numerical convergence. A convergence criterion based on the difference between the current and the previous iteration was employed and the solution is assumed convergent when this difference reached 10^{-5} in the present work. It should be mentioned that the convergence of the solution was initially dependent on the initial assumed solution and the step size. Numerical results for the velocity and temperature profiles for various fluid index coefficients are presented graphically in Figs 2 through 7 for the case of constant wall heat flux.

Figures 2 through 4 present typical profiles for the similarity function f, tangential velocity f' and temperature θ profiles for the similarity equations with the coefficients a_1, b_1, and c_1, given by Eq. (22) for various values of the fluid index coefficient n, respectively. It is clearly seen that as the fluid index coefficient n increases, both the fluid tangential velocity and the function f decrease while the fluid temperature θ increases. This is in constrast with what was is reported by Metha and Rao [1] for the same problem with non-isothermal power-law temperature distribution at the wall in which the temperature was decreased as n increased.

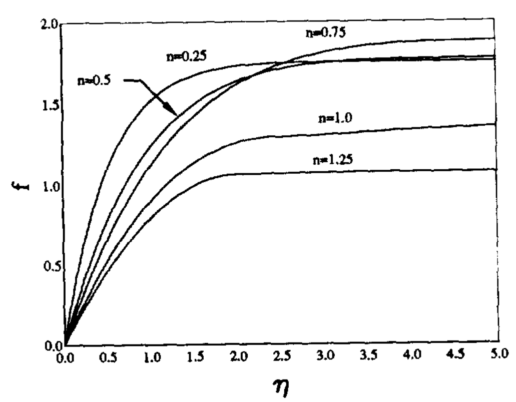

FIG. 2
Effects of n on f

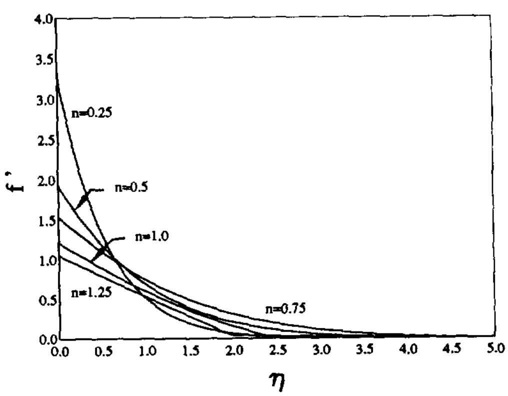

FIG. 3
Effects of n on Tangential Velocity Profiles

Figures 5 through 7 show profiles for f, f′ and θ based on the values of a_2 , b_2 , and c_2 given in Eqs. (23) for different values of n, respectively. Again, both the fluid velocity and the function f tend to decrease and θ increases over most of the region as n increases.

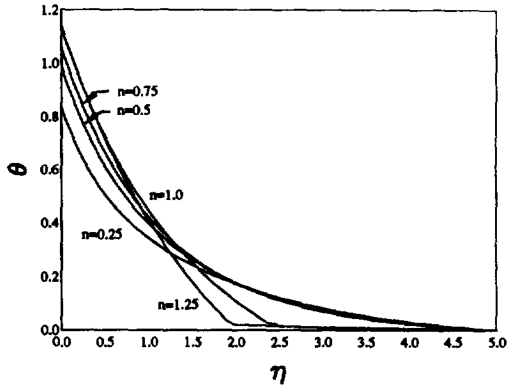

FIG. 4
Effects of n on Temperature Profiles

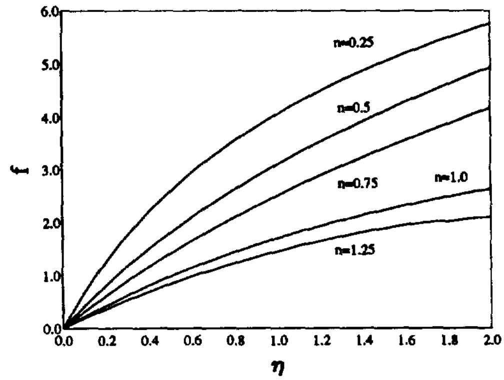

FIG. 5
Effects of n on f

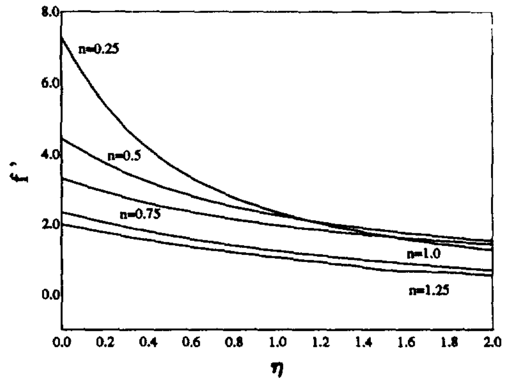

FIG. 6
Effects of n on Tangential Velocity Profiles

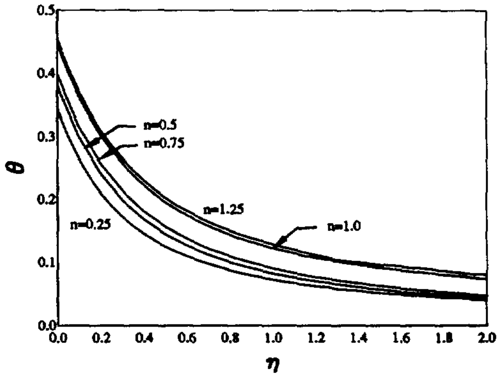

FIG. 7
Effects of n on Temperature Profiles

Finally, Table 1 shows a comparison between the values of the heat transfer rate $-\theta'(0)$ reported by Metha and Rao [1] for the case of power-law surface temperature distribution and the numerical results based on Eq. (20) of the same case . As is clearly shown from this table, excellent agreement between the results is observed. It should be mentioned that the numerical values for the work of Metha and Rao [1] were obtained by digitizing the graph of $-\theta'(0)$ they reported.

TABLE 1
Comparison of $-\theta'(0)$ values for non-isothermal wall temperature

n	λ	Metha and Rao [1]	Present Results
0.5	0	0.43073	0.44336
1.0	0	0.43323	0.44412
2.0	0	0.46039	0.46320
0.5	0.5	0.85558	0.85815
1.0	0.5	0.81943	0.82203
2.0	0.5	0.82257	0.82426
0.5	1.0	1.14478	1.15454
1.0	1.0	1.10370	1.11320
2.0	1.0	1.09800	1.10020

Conclusion

The problem of steady, laminar, buoyancy-induced flow of a power-law non-Newtonian fluid over a horizontal surface embedded in a uniform porous medium was formulated. A general similarity transformation was employed to transform the developed governing partial differential equations into ordinary differential equations. The conditions for similarity solutions are given for constant and variable power-law wall temperature distribution and constant wall heat flux. It was found that for the latter case there existed two possible different similarity equations. The similarity equations for each case were solved using an implicit, tri-diagonal, iterative finite-difference method. Very small step sizes were needed to produce a solution. Graphical results for the tangential velocity and temperature for the case of constant wall heat flux are reported. It was found that the fluid velocity decreased and its temperature increased as the fluid index coefficient was increased. The increase in temperature for the case of constant wall heat heat flux is contrast with the case of non-isothermal power-law temperature distribution in which the temperature decreased as the fluid index coefficient was increased. Excellent agreement with previously published work for the case of non-isothermal surface temperature distribution was obtained.

References

1 K.N. Metha and K.N. Rao, Int. J. Engg. Sci. **32**, 521, (1994).

2 P. Cheng and I. D. Chang, Int. J. Heat Mass Transf. **19**, 1267 (1976).

3 A. Nakayama and H. Koyama, Appl. Sci. Res. **48**, 55 (1991).

4 T. Govindarajulu and M.B. K. Moorthy, J. Energy, Heat and Mass Transf. **12**, 185 (1990).

5 A.J. Chamkha, Int. Commun. Heat and Mass Transfer. **23**, 875 (1996).

6 H.T. Chen and C.K. Chen, J. Heat Transf. **110**, 257 (1988).

7 H.T. Chen and C.K. Chen, Int. Commun. Heat and Mass Transf. **15**, 605 (1988).

8 A. Nakayama and H. Koyama, Heat Fluid Flow **8**, 240 (1987).

9 A.J. Chamkha, Fluid / Particle Separation J. **7**, 4(1994).

10 A.J. Chamkha, Fluid / Particle Separation J. **9**, 129 (1996).

11 R.H. Christopher and S. Middleman, Ind. Engng Chem. Fundam. **4**, 422 (1965).

12 R.V. Dharmadhikari and D.D. Kale, Chem. Engng Sci. **40**, 527 (1985).

13 A. Ridha, Int. J. Engng. Sci, **34**, 659 (1996).

14 F. Blottner, AIAA J. **8**, 193 (1970).

15 S.V. Patankar, Numerical Heat Transfer and Fluid Flow, McGraw-Hill Company, New York (1980).

Received February 25, 1997